

**INVESTIGATION OF OUTBURST CHARACTERISTICS IN  
DWARF NOVAE BINARY STAR SYSTEMS**

**FOR PARTIAL FULLFILLMENT FOR THE  
REQUIREMENTS OF THE MASTERS IN PHYSICS**

**BY:**

**JAMES STUART KLEP**

**ADVISOR: DR. RONALD KAITCHUCK**

**BALL STATE UNIVERSITY**

**MUNCIE, INDIANA**

**JULY 2009**

## ABSTRACT

**THESIS:** Investigation of outburst characteristics in dwarf novae binary star systems.

**STUDENT:** James Klep

**DEGREE:** Master of Science

**College:** Science and Humanities

**DATE:** December, 2009

**PAGES:** 58

Dwarf novae are a type of binary star system that consists of a cool red dwarf, as well as a white dwarf with an accretion disk. Occasionally the disk will get significantly brighter for a few days in an event called an outburst. On February 6<sup>th</sup>, 2002 one such system, CN Orionis, was experiencing such an outburst. The goal of this research was to determine some important characteristics of CN Orionis during its outburst. This thesis will present the light output, temperature, and the area of the accretion disk of CN Orionis.

## **Acknowledgements**

The author would like to thank his research advisor, Dr. Ronald Kaitchuck for his guidance, patience, and for putting up with the author's general tomfoolery. The author would also like to thank the Department of Physics and Astronomy at Ball State for all of their support during this research.

# Table of Contents

<b>Ch 1</b> Introduction	pg. 1
<b>Ch 2</b> Novae Types	pg. 5
Supernovae	pg. 5
Novae	pg. 9
Dwarf Novae	pg. 10
<b>Ch 3</b> Dwarf Novae Systems	pg. 13
Origin	pg. 13
Accretion Disk and Outbursts	pg. 16
Outburst Shapes	pg. 22
Superoutbursts and Superhumps	pg. 24
<b>Ch 4</b> Background	pg. 28
Reduction Process	pg. 31
Bias Frames	pg. 32
Dark Frames	pg. 33
Flat Field Frames	pg. 34
Photometry	pg. 35
Differential Photometry	pg. 36
Extinction	pg. 37
Transformation Coefficient	pg. 39
Blackbody Fitting	pg. 41
<b>Ch 5</b> Results	pg. 45
CN Orionis	pg. 45
Observations	pg. 46
Differential Photometry	pg. 47
Temperature	pg. 52
Area Ratio	pg. 53
Conclusions	pg. 55
Bibliography	pg. 57

**List of Tables**

Table 1.	Modified Ritter Catalog	pg. 3
Table 2.	Basic Properties of Novae	pg. 12

## List of Figures

Figure 1.	Onion Skin Model	pg. 8
Figure 2.	Roche Lobes	pg. 15
Figure 3.	S-Curve Model	pg. 19
Figure 4.	Outburst Shapes	pg. 22
Figure 5.	Lightcurve of VW Hyi	pg. 24
Figure 6.	Average normalized magnitude for SS Cyg (15 days)	pg. 29
Figure 7.	Average normalized magnitude for SS Cyg (8 days)	pg. 30
Figure 8.	Lightcurve of SS Cyg	pg. 30
Figure 9.	Airmass Diagram	pg. 38
Figure 10.	Lightcurve of CN Ori	pg. 46
Figure 11.	Differential Photometry (B Filter)	pg. 48
Figure 12.	Differential Photometry (V Filter)	pg. 49
Figure 13.	Differential Photometry (R Filter)	pg. 50
Figure 14.	Differential Photometry (I Filter)	pg. 51
Figure 15.	Temperature vs. Time	pg. 52
Figure 16.	Area Ratio Graph	pg. 54

# Introduction

Most stars live their life on the main sequence at a constant brightness. However, some stars called variable stars can appear to change brightness with time. Most of the variable stars observed are either too dim to see or their changes are too subtle to be noticed by the unaided eye. Dwarf novae (DN) are a classification of variable stars, but how and why they vary sets them apart from other variables. While most variable stars have a well-defined period which makes their observations easier, dwarf novae on the other hand are rather unpredictable. The reasoning behind the irregularities is not fully understood and the work presented attempts to understand more about what occurs in a dwarf nova system in the stages before the system brightens. Earlier work at Ball State University showed that peculiar patterns might occur in the days preceding an outburst in the well-known dwarf nova SS Cyg. Such precursors to an outburst can be useful in giving an advanced warning that an outburst is imminent. The goal of this research was to determine whether or not these patterns exist in other dwarf nova systems, or

if these patterns were due to the uncertainties in the data that was collected over time. This thesis concentrates on CN Orionis, a fast period system in the constellation Orion. The data collected for this work were taken with the 31-inch telescope at the National Undergraduate Research Observatory (NURO) in Flagstaff, AZ in February of 2002 and reduced using the Image Reduction and Analysis Facility (IRAF) package. Photometry was done using CCDRED and CCDPHOT.

Figures 6 and 7 in Chapter 4 show a possible flickering in magnitude a few days before the outburst of SS Cyg. In order to determine if the flickering is present, SS Cyg could be observed with more accurate instruments. However, SS Cyg has an outburst interval of 24-63 days. So in order to improve the chances of seeing these pre-outburst patterns, it would be necessary to choose a system with a short outburst interval.

The sixth edition of the Ritter Catalog [Ritter 1997] lists 318 cataclysmic binaries, 47 low mass X-ray binaries, and 49 other related objects. In some cases the catalog lists the outburst intervals for the entries and from this list a catalog of stars suitable for observation was created (Table 1). The Ritter Catalog was modified by removing anything that was not a dwarf nova system. Any dwarf nova that had an average outburst period greater than 20 days or was unknown was cut from the list. The final



result is a listing of 22 objects out of the original 414 that are short outburst interval dwarf novae systems that would be suitable for this project and is included with this thesis.

The project was to look at data previously taken for the star CN Ori at NURO in early February of 2002. During this study the system was undergoing an outburst and the characteristics of the system were studied in four color photometry, which at the time of this writing has not been done for CN Ori.

### **Modified Ritter Catalog**

<b>Name</b>	<b>RA</b>	<b>Dec</b>	<b>Outburst Interval (Days)</b>
RX And	01 04 35.6	+41 17 58	17
FO And	01 15 32.1	+37 37 36	15-23
AM Cas	02 26 23.4	+71 18 32	8
V1159 Ori	05 28 59.5	-03 33 53	4
CN Ori	05 52 07.8	-05 25 01	18
HL CMa	06 45 17.0	-16 51 35	17
SV CMi	07 31 08.4	+05 58 49	16
BX Pup	07 54 15.6	-24 19 36	18
YZ Cnc	08 10 56.6	+28 08 34	6-16
AT Cnc	08 28 36.9	+25 20 03	16
DI Uma	09 12 16.2	+50 53 55	4

<b>Name</b>	<b>RA</b>	<b>Dec</b>	<b>Outburst Interval (Days)</b>
ER Uma	09 47 11.8	+51 54 09	4-5
RZ LMi	09 51 49.0	+34 07 25	3.8
HS Vir	13 43 38.4	-08 14 03	8
CR Boo	13 48 55.3	+07 57 35	4-8
NY Ser	15 13 02.3	+23 15 08	6-9
SS UMi	15 51 22.2	+71 45 12	11
IX Dra	18 12 31.4	+67 04 46	3-4
V344 Lyr	18 44 39.2	+43 22 28	13-19
MN Dra	20 23 38.3	+64 36 27	7-8
V503 Cyg	20 27 17.4	+43 41 23	7-9
VW Vul	20 57 45.1	+25 30 26	14-23

*Table 1: Modified Ritter Catalog listing only short outburst period dwarf novae.*

## **Novae Types**

### **Supernovae**

Most people are familiar with the term supernova that refers to the most luminous and longest lasting type nova. They are able to outshine their host galaxy and their brightness lasts for months before dimming. A supernova occurs as the end result of a star that is greater than three times the mass of our Sun, meaning that our Sun will never go supernova in its lifetime [Zeilik and Gregory 1998]. Supernovae are considered variable stars since the light output of the star changes, even if it only happens once. It is unfortunate that they are also rather rare in our Galaxy, with the last observation of a supernova being before Galileo's use of the telescope, making the study of supernovae rather difficult. So any observations done on supernovae are done in other galaxies. A star that will eventually become a supernova start out on the main sequence fusing hydrogen into helium, just like any other main sequence star. They are generally massive, blue, and have very high surface temperatures. High mass stars never last very long on

the main sequence even though they have a large starting mass. The important thing is the rate at which high mass stars convert their fuel into heavier elements. Stars of this nature can consume their fuel in a short amount of time. For comparison purposes our Sun, being at one solar mass, in the middle of its total life span, will run out of hydrogen fuel in about five billion years. For a star of 25 solar masses the lifetime will be only roughly six million years. Once the core consumes its hydrogen fuel the star will no longer be in equilibrium. The outward photon pressure due to fusion in the core will no longer balance the pressure due to its own gravity of the gas above the core. As a result the core will begin to contract. The core will increase in temperature from the compression until the conditions are right for the helium atoms that have been produced to begin fusing and releasing energy. This will then halt the collapse of the core and the process starts all over again. But there is a caveat to this. The core is now much hotter than before, therefore the star will fuse helium at a higher rate. It has to do this because the energy output for the fusion of helium is less than hydrogen. In order for the star to be in equilibrium more fusion reactions must occur in order to counter gravity; therefore the time the star stays at this stage in its lifecycle is shorter still. This process of using a fuel, compressing to ignite the next element will repeat until the star will have layers of elements

stacked up around an iron core. This “Onion Skin” model (Figure 1) is what the star’s interior looks like before it goes supernova [Karttunen 2000]. Iron turns out to be the most stable element and any attempt to fuse iron atoms together will result in a deficit in energy. What triggers the actual supernova is the collapse of this iron core. The iron atoms will disassociate into protons, neutrons, and electrons releasing an enormous amount of energy and neutrinos [Zeilik and Gregory 1998]. The released energy will go into the outer layers of the star, creating elements that are heavier than iron up to uranium via neutron capture. The protons and electrons in the core will combine, forming neutrons so that the core is essentially one big nucleus. And depending on the initial mass of the star, the remnants of a supernova could be a neutron star as described above or for the most massive stars a black hole is produced. The process described above takes an extraordinarily short amount of time compared to the lifetime of the star, on the order of a few seconds for the supernova to start [Zeilik and Gregory 1998].

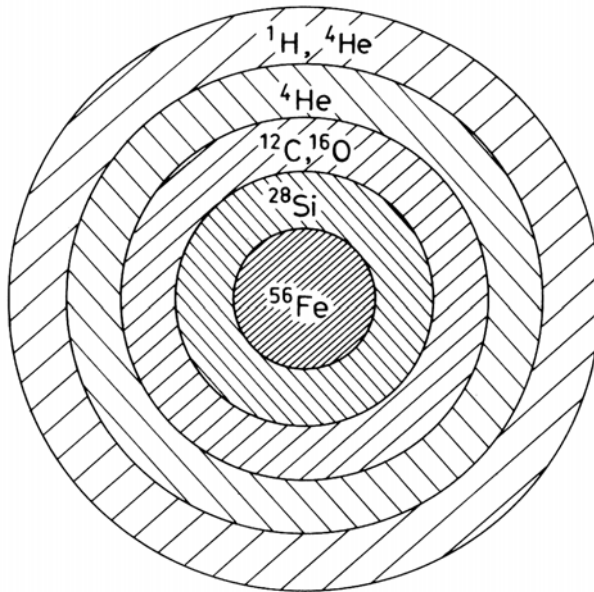


*Figure 1: Onion Skin Model of a massive star that will eventually go supernova*

There's also another way to produce a supernova. This would involve a white dwarf with a companion star that accretes material onto the white dwarf. This continues until the mass of the gas, plus the mass of the white dwarf will be greater than the Chandrasekhar Limit of 1.4 solar masses and the core will undergo the same collapse to a neutron star and will explode as a Type I supernova. Since these types of supernovae always occur when the Chandrasekhar Limit is breached the mass will always be 1.4 solar masses. This means that the energy output from Type I supernovae are the same and thus can be used to measure distances, especially to distant galaxies.

## Novae

Regular novae are different from supernovae in the mechanism and the physical makeup of the system and how they become more luminous. As the name implies, the increase in luminosity is much less than that of a supernova. A nova system consists of a white dwarf and either a main sequence or more evolved star as a companion orbiting around a common center of mass. As with some systems of this nature, the gas from the companion star's envelope will flow towards the white dwarf. This will form an accretion disk around the white dwarf in order to conserve angular momentum. The gas will not be static in this disk as frictional forces steal energy from the gas, causing it to draw closer to the white dwarf.

Eventually the pressures, temperatures and densities will become sufficient for the gas to ignite and fuse the hydrogen into helium at the stellar surface. These nuclear reactions will cause further nuclear reactions, creating a runaway reaction to occur until the layer of degenerate gas on the surface expands violently. This violent reaction releases light that is recorded as a nova [Zeilik and Gregory 1998]. The process then happens all over again so there is some periodicity to a novae system, generally tens of thousands of years between outbursts.

Novae aren't nearly as bright or energetic as supernovae. A nova can increase its brightness up to 1600 times, releasing as much as  $6 \times 10^{37}$  Joules of energy. A supernova can get at least  $1 \times 10^8$  times brighter and release  $10^{44}$  Joules of energy.

## **Dwarf Novae**

Dwarf novae are the weakest of the three systems and are the focus of this thesis. Dwarf novae are similar to novae in that they are binary star systems, but with important differences. A dwarf nova system will consist of a white dwarf and a main sequence red dwarf. Like novae systems, they will have an accretion disk around the white dwarf. The similarities end as the mechanism in which an outburst occurs. As the material in the disk spirals towards the white dwarf it will dam up within the disk. As more gas from the companion star accretes into the disk, temperatures and pressures rise until conditions are sufficient to "break the dam" and flush the disk of its excess material onto the surface of the white dwarf. Energy is released as the material goes from a higher gravitational potential energy to a much lower potential, releasing light and thus an outburst. The whole process starts over again and depending on the system a dwarf novae can spend as little as a few



days or as much as a few decades in quiescence. This simplistic explanation of a dwarf nova is expanded in the next chapter.

Dwarf novae are further broken down into three subtypes based on the characteristics of the outburst:

*Z Cam*: Outbursts from *Z Cam* stars have a plateau about 0.7 magnitude below maximum. Afterwards the system returns to pre-outburst brightness for weeks to years before the next outburst;

*SU UMa*: These stars occasionally experience a superoutburst where the maximum brightness increases by about 0.7 magnitude. This maximum brightness is then sustained for roughly five times longer than a typical outburst;

*U Gem*: A *U Gem* star is simply any system that can't be categorized as *Z Cam* or *SU UMa* [Warner 2003].

As the name implies the energy output is weaker compared to the classical novae, with the dwarf novae getting about 40 times brighter at the peak of outburst.

Table 2 gives an overall summary of the characteristics of the types of novae discussed. [Zeilik and Gregory 1998]

Type	$M_{\max}$	$\Delta M$	Energy per Outburst (J)
Supernovae I	-20	>20	$10^{44}$
Supernovae II	-18	$\sim 14$	$10^{43}$
Novae (Fast)	-8.5 to -9.2	11 to 13	$6 \times 10^{37}$
Novae (Slow)	-5.5 to -7.4	9 to 11	----
Novae (Recurrent)	-7.8	8	$10^{37}$
Dwarf Novae	+5.5	4	$6 \times 10^{31}$

Type	Cycle	Mass Ejected/Cycle (Solar Masses)	Velocity of Ejection (km/s)	Mass of Star (Solar Masses)
Supernovae I	N/A	$\leq 1$	10,000	1
Supernovae II	N/A	?	10,000	$\geq 4$
Novae (Fast)	$\sim 10^6$ years	$10^{-5}$ to $10^{-3}$	500 to 4000	1 to 5
Novae (Slow)	N/A	N/A	100 to 1500	0.02 to 0.3
Novae (Recurrent)	18 to 80 years	$5 \times 10^{-6}$	50 to 400	2
Dwarf Novae	40 to 100 days	$10^{-9}$	N/A	$\sim 0.4$

Table 2: Basic properties of all three novae systems

# Dwarf Novae Systems

## Origin

The following section details how two stars, starting far apart, eventually come closer together to form a close binary star system as well as describing the evolution that takes place after the system becomes stabilized. Hellier (2001) is the primary reference for this section.

A dwarf nova system can easily fit inside the volume of our own Sun but the evolution of such a system will have the two stars starting very far apart. Binary star systems are comprised of a lower mass, secondary, star and a higher mass, primary, star. In the case of dwarf nova systems the primary is greater than one solar mass and the secondary less than a solar mass. If we were to consider the lines of gravitational equipotential for a particle at rest in the binary star system, we would see that close to the stars themselves the equipotential would be spherical and concentric. Further out the lines start to become distorted. This distortion arises from the gravitational influence of the other star but also from the centrifugal forces

that arise if the system is in a co-rotating reference frame. Once the equipotential lines are drawn, one aspect that would be noticed is a point of intersection. The point where the lines cross between the two stars is the Lagrangian point. Other Lagrangian points do exist in binary systems but the one between the two objects is the one of interest. The significance of this Lagrangian point is that any test mass at this point in the co-rotating reference frame will not fall toward either star. The lines of gravitational equipotential also create what are known as Roche Lobes. A Roche Lobe is defined as an area of space where a test mass would fall towards that particular object if it were located within its lobe. Figure 2 [Cornell 2009] shows both stars centered on their respective Roche Lobes and the Lagrangian point between the two. The process of stellar evolution causes the more massive star to begin aging much sooner than the less massive companion star. One consequence of this is that as the star ages it will begin to expand, filling its Roche Lobe and crossing the Lagrangian point.

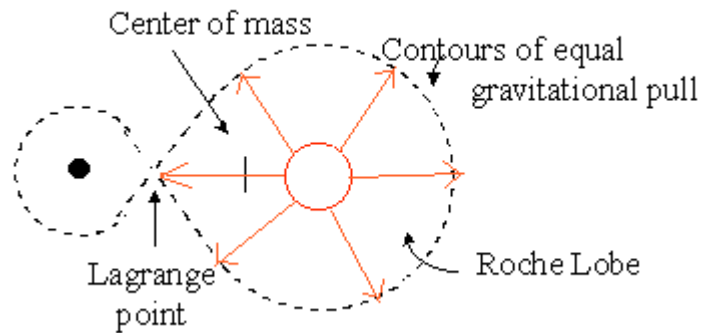


*Figure 2: Binary star system and equipotential lines*

Once the expansion passes the Lagrangian point the outer gas begins to transfer to the companion star as a stream of material as the gravitation attraction to the white dwarf is much greater than the gravitation pull of the original star. When this occurs the system becomes since because angular momentum must be conserved. As the gas falls towards the companion star, it gains angular momentum. The system must then compensate for this extra momentum by drawing the two stars closer together. This causes the Roche Lobes to shrink, causing even more material to spill over onto the companion and drawing the stars closer still. Eventually both stars will be close enough to form a common envelope so that both stars appear as a peanut shaped configuration. The secondary in this configuration experiences a drag resistance as it orbits inside the red giant. The drag robs the orbital energy and angular momentum from the secondary and causes the

system to shrink further. The system stays this way, assuming no collisions or gravitational interactions from outside objects. However, gravitational radiation that arises from Einstein's General Relativity and magnetic braking causes the two stars to draw closer but at very long time scales.

Magnetic braking is thought to occur as charged particles from stellar winds are shot along magnetic field lines, gradually removing some angular momentum from the system as the particles make a very long lever arm. Both of these processes are very slow. As the system stabilizes it takes these forms of braking a very long time to have any noticeable effects.

## **Accretion Disk and Outbursts**

This section describes what goes on in the accretion disk during an outburst as well as the evolution of the disk before, during, and after the outburst occurs. The sources for the section are Cannizzo and Kaitchuck (1992) and Hellier (2001).

Once the system has a stable configuration with the white dwarf and a cool, red star orbiting each another in close proximity with an accretion disk around the white dwarf an outburst may occur. Within the disk is an area where the material from the secondary is slamming into the disk. This region, called the hotspot, can be hotter and brighter than the other

components of the system combined [Warner 2003]. The secondary, being a red dwarf, does not have the luminosity due to its low temperature. The white dwarf, although hot, is very small and will not contribute much to the light output of the system. The definition of an outburst is when the system rapidly brightens then returns to its original brightness. It is this type of outburst that make dwarf novae unique. The outbursts of a dwarf nova rarely, if ever, happen at regular intervals. This makes studying dwarf novae all the more difficult, especially when the data needed is dependent on where the system is in its outburst cycle. The time it takes to go from quiescence to the maximum brightness is usually different from outburst to outburst.

So the question that naturally arises is what is going on in the system? Why does it suddenly get brighter? There are two theories that attempted to answer this question. The first theory is more intuitive and suggests that an outburst would occur if there was a sudden burst of material flowing from the secondary and accreting onto the white dwarf. This would result in more light being emitted from the system as a change in gravitational potential energy. The second theory was formulated by Yoji Osaki. He suggested that the instability occurred within the accretion disk itself [Mineshige 1983]. He suggested there were times when the rate that material flowed onto the white dwarf didn't match the rate at which material flowed into the accretion disk

from the secondary. This would make the disk unstable and eventually clear the gas out of the disk, causing the system to glow brighter. The observational evidence greatly favors Osaki's disk instability model. However, the first theory hasn't been completely discredited and may play a supporting part in outbursts [Smak 1984].

So what is going on in the accretion disk itself that causes it to become unstable? For the white dwarf system, a great majority of the mass is in a central object so that the disk rotates in a Keplerian way, meaning that gas closer to the central object orbits faster, but has a lower angular momentum. Gas farther out orbits slower but have a greater angular momentum. As mentioned earlier, the amount accreting material onto the white dwarf is not the same amount that is being supplied by the companion. So somewhere in the disk there will be a backlog of gas. This backlog causes adjacent gasses to experience a greater frictional force as inner gasses orbits faster. When this occurs the gas loses some energy and must spiral closer to the white dwarf. This process is defined as the viscosity. It then raises the temperature until conditions are sufficient enough to cause this backlog of material to start the outburst.

The previous passage is best described in an S curve graph that explains how the outburst mechanism works. Figure 3 shows a plot of



temperature versus  $\Sigma$ , which denotes the surface density for an annulus in the disk. The other y-axis shows the state of the gas within the disk. In reality there is more going on in the disk than the graph suggests. Either y axis could be replaced with other parameters such as the opacity, amount of mass moving through the annulus, or how the viscosity changes. Therefore, there is a lot more going on than Figure 3 would suggest in terms of the physics going on in the system. In quiescence the annulus is along the lower branch, between points A and B, and when in outburst the annulus is along the upper branch, between D and C [Hellier 2001].

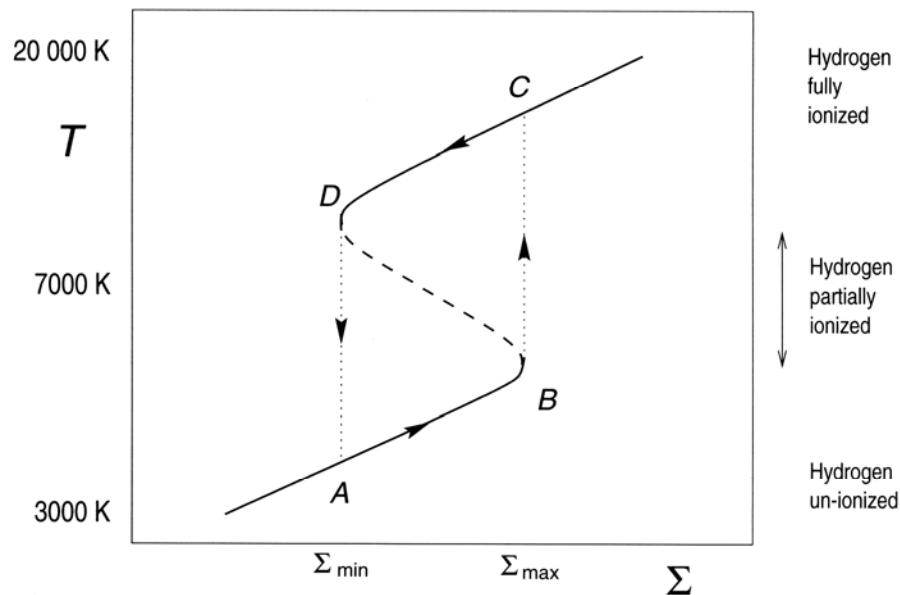


Figure 3: S-Curve Model. Note this is the solution for one annulus of partially ionized hydrogen in the disk and not for the entire disk

Starting at point A the disk gradually fills with material from the secondary, this in turn increases the surface density and thus the temperature

as frictional heating increases. Eventually when the annulus gets to point B something interesting happens. The annulus becomes unstable and essentially the disk begins to go into outburst.

The points between B and C are considered unstable due to the opacity of the gas. Opacity is defined by how well photons can get through a substance. So substances like water or glass will have a low opacity while muddy water or highly tinted glass will have a higher opacity. In the accretion disk the only material that is available is hydrogen gas. It turns out that the opacity of hydrogen gas is very low when all the electrons are combined with nuclei to form a neutral element. Inversely, the opacity is very high when the material becomes partially ionized or if there are  $H^-$  ions, a proton with two electrons orbiting, as they are very eager to interact with photons. In fact  $H^-$  ions are the driving factor in all outbursts.

Between the two extremes the gas is a mixture of ions and neutral atoms and it is at this state that the annulus is thermally unstable. When the gas is partially ionized, any energy that is added goes into creating more ions rather than increasing the temperature. This makes the opacity very sensitive to any increase in temperature such that the opacity goes as  $T^{10}$  and it is this sensitivity that that triggers the outburst.

Between points B and C most of the energy goes into creating ions and raising the opacity of the gas. This traps the photons, raising the temperature, creating more ions till the gas becomes fully ionized. When this occurs the opacity loses the extreme sensitivity to the temperature and the disk is at point C.

At point C the viscous interactions are very strong, robbing the annulus of angular momentum. As a result the material starts to flow quickly onto the white dwarf. Naturally, the annulus loses surface density and therefore also cools, as there would be less material in the disk. The annulus then travels from points C to D. At point D the radiation losses overwhelm any heating from the viscosity. The opacity of the annulus drops as the temperature decreases until it reaches point A and the annulus returns to quiescence. Here the outburst cycle has come full circle and starts all over again.

All of this doesn't happen throughout the disk at an instant. The above s-curve applies to one annulus in the disk so when one annulus reaches the critical maximum surface density and starts to rapidly raise in temperature it will influence the neighboring annuli. Where that occurs is dependent on the rate at which material from the secondary is transferred to the disk. If the rate is rather slow, then material will have time to spiral towards the white

dwarf and the backlog will occur at smaller distances away from the white dwarf. If the opposite is true, and there is a faster rate of transference, then the backlog occurs at larger radii out since the material will not have time to migrate towards the white dwarf. This means that depending on the rate of accretion the system experiences an inside-out outburst for slow rates, and an outside-in outburst for fast rates.

## Outburst Shapes

Figure 4 [Hellier 2001] shows the light curve that can be formed from a dwarf nova outburst while Figure 8 shows the light curve for the well-known dwarf nova SS Cyg. Right away one can see that the shapes vary between subsequent outbursts. This section explains how these shapes form during an outburst.

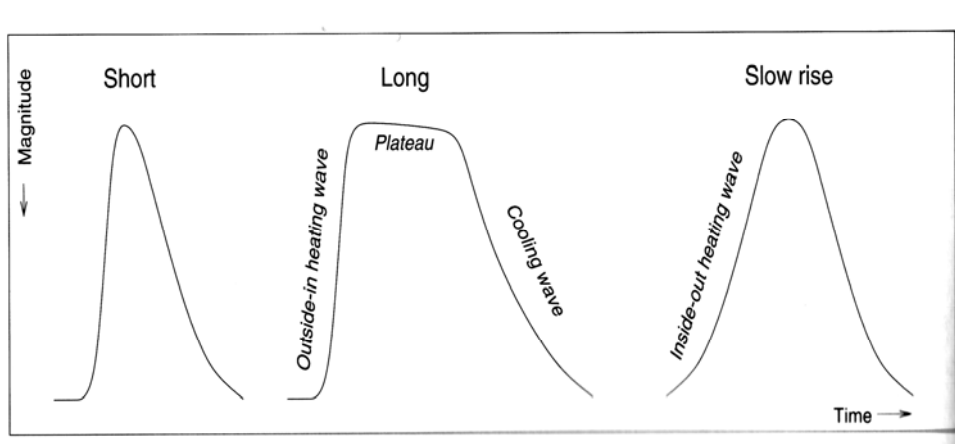


Figure 4: Three types of outburst shapes that occur

The first shape has a very steep slope as the outburst occurs. This happens because the annulus responsible for starting the outburst lies near the outer edge of the disk. When the viscosity rises in the outer edge the material will flow inwards. This in turn increases the surface density of the next annulus, causing it to reach the non-stable point on the S curve. This sets up a domino effect for the disk thus making the outburst occur very rapidly.

Next are outbursts that rise rapidly, but the outburst itself lasts longer than normal. The rapid rise is due to the same reason as discussed in the first outburst pattern where the domino effect in the disk causes a rapid increase in disk brightness but the maximum light output is sustained for a longer period of time. Finally, there are the outbursts that are more symmetric in shape. The slower rise time occur because the annulus responsible for starting the outburst is much closer to the white dwarf. The inner radii have a more difficult time influencing the outer radii into outburst, causing the rise time to be much slower than that of an outside-in outburst. In all three cases the slope to end the outbursts are all the same. This is due to the mechanism stopping the outburst always occurring in the outer part of the disk no matter where it started.

## Superoutbursts and Superhumps

Figure 5 shows a three-year light curve for the system VW Hyi. As well as having regular outbursts that last for a few days, the figure also shows signs of longer outbursts with the maximum output being slightly higher than a normal outburst. Such outbursts are known as superoutbursts and are a feature of SU UMa systems. The general reference for this section of the thesis is Hellier (2001).

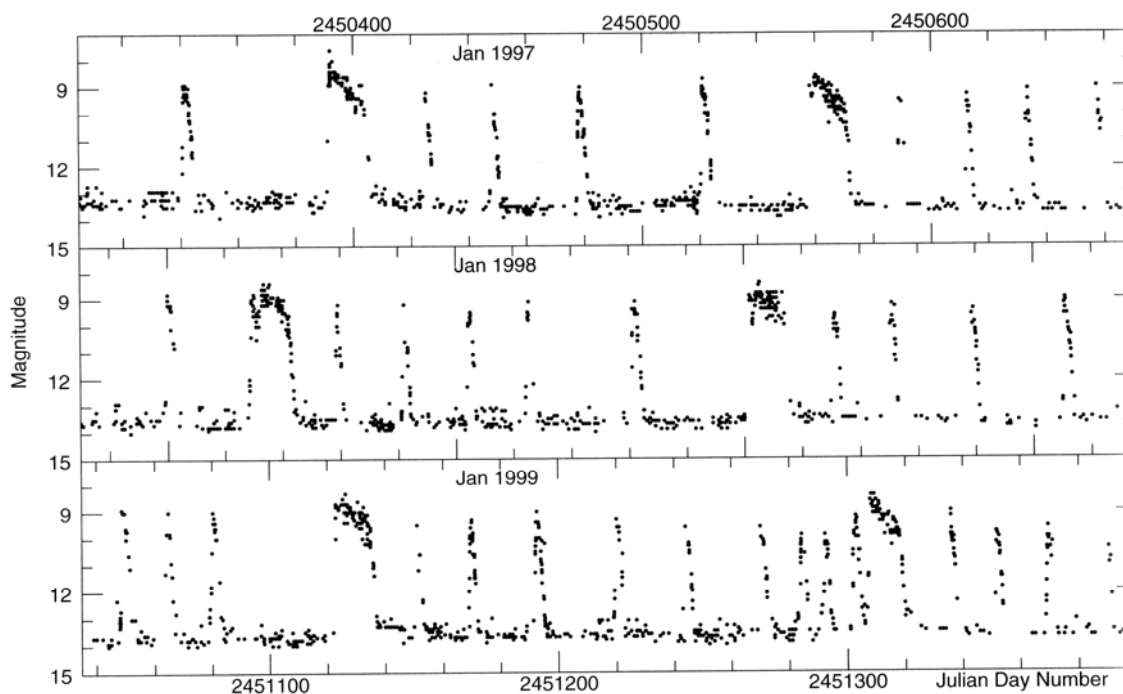


*Figure 5: Three year light curve of VW Hyi that features both normal outbursts and superoutbursts*

Figure 5 also shows that superoutbursts are periodic, with a period called a supercycle. Further examination reveals that within the

superoutburst is a periodic function that occurs near the maximum brightness of the outburst. This feature, called a superhump, is a little longer than the orbital period of the novae system. The reasons for this are still under some debate [Osaki & Meyer 2004, Smak 2009]. The accepted theory is that the geometry of the accretion disk changes during an outburst. Figure 3 shows that with the onset of an outburst the temperature of the disk grows rapidly. This is due to the gaseous nature of the disk as it expands with an increase in temperature. As the disk size increases there is more gravitational influence from the secondary. As a result, the portion of the disk that is closer to the secondary bulges out somewhat and the outer disk becomes more elliptical than annuli closer to the white dwarf. This results in adjacent annuli not being parallel in their orbits and thus some orbiting gas intersects a neighboring orbit. This increases the light output and is added to the overall energy output caused by the thermal instability of the disk for a regular outburst. The extended time of the outburst arises from the tidal stresses on the disk that increase the angular momentum of the disk. And again, in order to conserve angular momentum, there must be an enhanced flow of matter from the disk towards the white dwarf that allows the disk to sustain its outburst state.

Another theory arises due to the elliptical disk model's inability to explain some observational results, namely the amplitude of superhumps [Smak 2009]. The idea of this theory is that an eccentric disk doesn't cause the superhumps but the extra radiation onto the companion star from the white dwarf and disk causes extra material to flow through the Lagrangian point of the system [Smak 2004].

The origin of the superhump arises from the elliptical annulus of the accretion disk precessing. This means that the time it takes the major axis of the elliptical annulus to orbit the white dwarf is different than the orbital period of the binary star system. Because of the discrepancy between the two orbital periods, the elongated annulus is not in the same position after one orbital cycle. To further understand this we take the initial position of the elongated annulus to be lined up with the secondary. This configuration will have a certain brightness. The secondary is then allowed to orbit once around its companion, leaving the secondary back where it started. Precession of the elliptical annulus will not be in the same place however, it will be further into its own orbit. So, in order to return to the original brightness, the secondary has to move a little more into the orbit. This causes the period of the superhumps to be a few percent larger than the orbital period of the system. This all however does not explain why superoutbursts



do not occur with every outburst. Instead they occur after a number of outbursts have past. The argument is that every outburst leaves the disk with a little mass leftover. After a number of outbursts, the mass density in the disk is enhanced enough from the previous outbursts for a superoutburst to occur.

## Background

Figures 7 and 8 show the light curve for SS Cyg, a well-known dwarf nova system, and is often studied by amateur astronomers due to its brightness. There is an advantage to having thousands of amateur astronomers who look at the sky and observe several different objects creating very large databases. In the case of SS Cyg, much of the data that has been collected on the system is readily accessible at the American Association of Variable Star Observers (AAVSO). There is, however, a drawback to amateur observations. The disadvantage is that most of these astronomers are using their eye to estimate the relative brightness of the variable star by using field stars of known brightness. The human eye just can not detect very small changes in the light output that can occur in a dwarf nova system during the binary star's outburst cycle. This, in turn, makes the data very scattered and somewhat less useful. Amateur observation is starting to change as the price of CCD cameras begins to drop. Like all technology, it allows more amateurs to purchase them and

make more useful observations. Nonetheless, it was using the 100+ years of observational data from amateur astronomers that has laid the groundwork for this thesis.

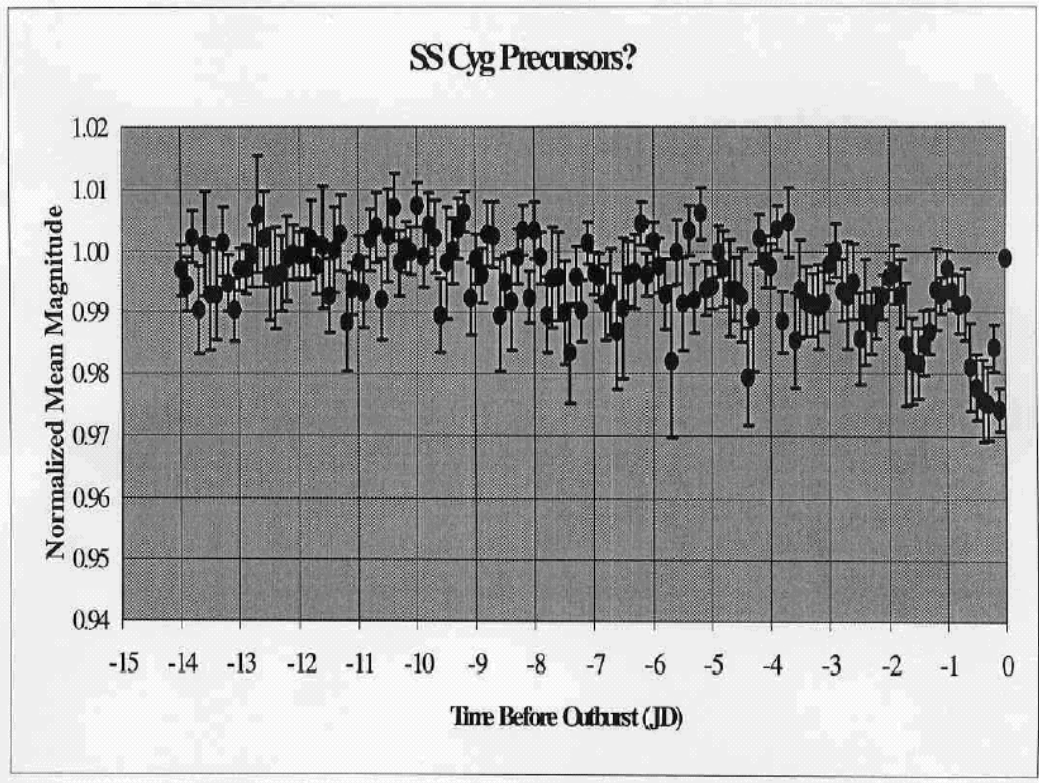


Figure 6: Average normalized magnitude for SS Cyg; note the sinusoidal motion two days before outburst

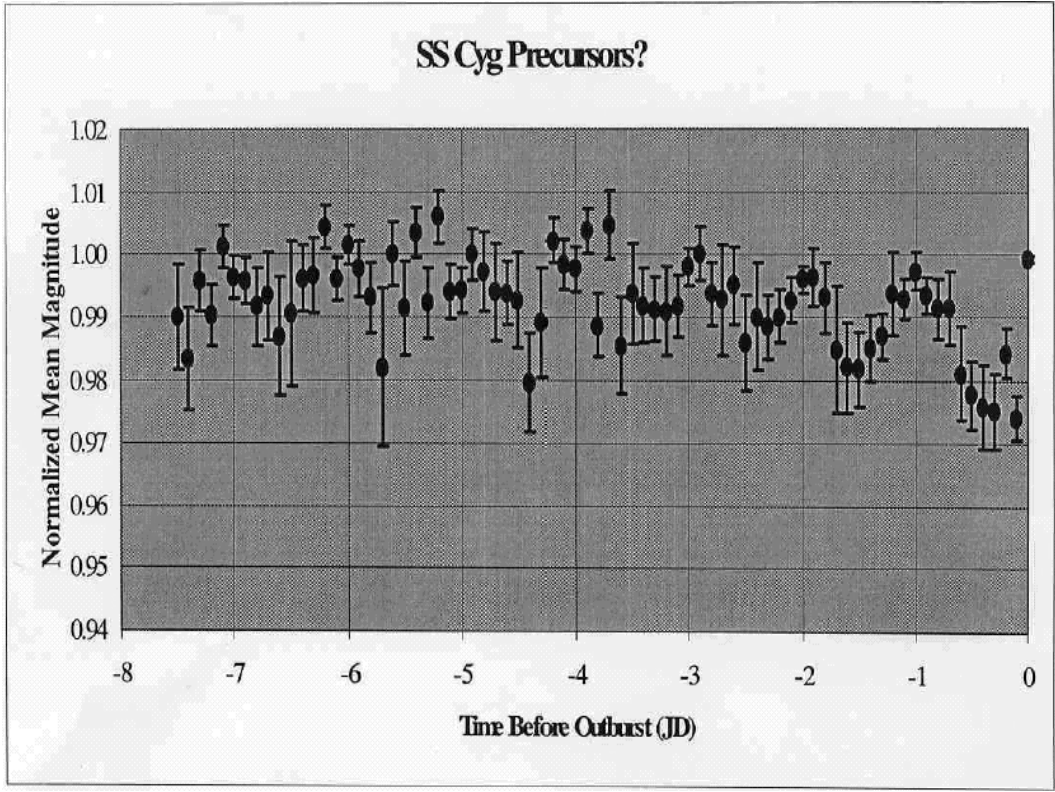


Figure 7: Similar chart to Figure 6, note the large error bars due to amateur observations

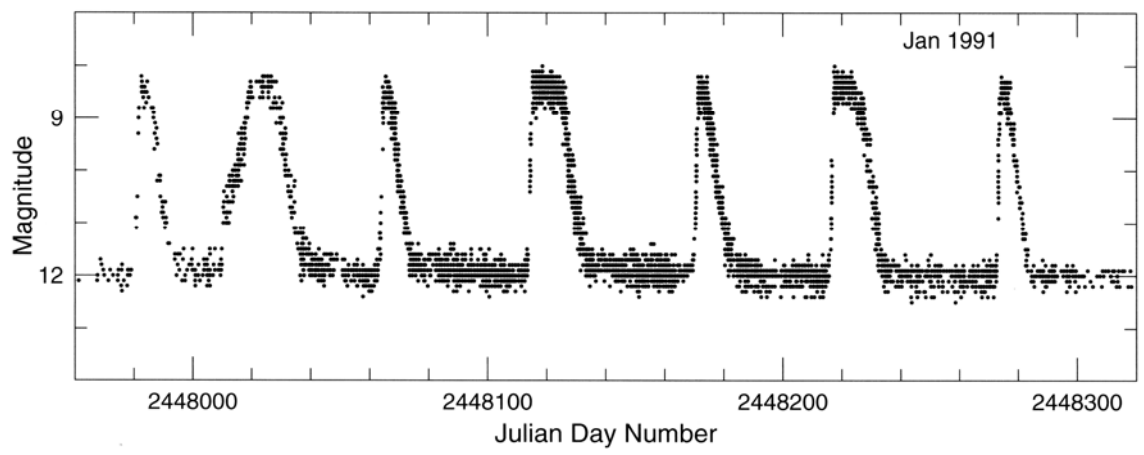


Figure 8: Magnitude vs. Julian Day Number plot for SS Cyg  
From origin to the end measures one full year

Bob Hill of Ball State University worked on all the data from AAVSO regarding SS Cyg. His findings are shown in Figures 6 and 7 that plot

average magnitude verses the number of days before an outburst. As the graphs show, there is a small oscillation about three to four days just before SS Cyg goes into outburst. This suggests that the system might “flicker” a bit before the actual outburst. However, it should be stressed that this was all done by amateur astronomers making their best estimate on the magnitude. By using more sophisticated technology of modern CCD cameras one can reduce the error so that accurate conclusions can be made on the nature of these patterns.

## **Reduction Process**

Like all forms of data there are corrections that need to be accounted for before any science can be done with them. There are three corrections that need to be taken with CCD images. These are bias subtraction, flat field division, and dark current subtraction. Each frame will be described below, showing how they are taken, why they are needed, and what IRAF does with them in the reduction process. For the sections on the different frames used in the reduction process the primary reference is Howell (2000). The section that deals with photometry Henden and Kaitchuck (1982) is the primary reference.

## Bias Frames

If one were to graph output signal vs. incident photons it should show that if there are no photons incident, the output would be zero as well.

Reality, however, shows that at zero input light there is still an output value.

This discrepancy is known as the offset bias and must be corrected. The source of this bias is from the on-chip amplifiers. In order to measure this offset an observer would take a zero second exposure with the shutter closed.

Generally the observer(s) take a series of bias frames at the beginning and end of the night. This will average out the occasional cosmic ray that hits the CCD, and read noise variations that could occur in any single bias image.

During the data reduction phase IRAF computes a master bias by taking one pixel from every bias frame and averaging them. They must be the same pixel location otherwise this process would be moot. For example, if an observer takes two bias frames and creates a master bias, IRAF will take pixel one from bias frames one and two, average their numbers and that will be pixel one for the master frame. Finally, the pixel values are subtracted from each object frame of interest in the final stages of data reduction. It should be noted that due to the nature of a bias is wavelength independent.

## Dark Frames

The primary material for a CCD chip is silicone, a semi conductive material that turns conductive at higher temperatures when most of the electrons fill the conductive band. Since the CCD chip is now somewhat conductive it will have many electrons moving about. This in turn creates extra current since the electron-hole pairs are similar to electron-hole pairs that are created from photons being incident on the CCD, thus making them indistinguishable. In order to reduce the effect of these thermally induced currents it is best to run the CCD camera as cool as possible. During an observation an observer takes a series of dark frames throughout the night. IRAF then averages the pixels much in the same way that it deals with the bias and flat-frames to create a master dark frame.

Dark frames are not really important to astronomers who use liquid nitrogen cooled cameras. Cameras that use liquid nitrogen can cool the CCD chips to about 80K. At these temperatures, the noise created from the electrons is minimal, making a dark frame with these cold cameras just a very long bias frame.

## Flat Field Frames

The next series of images to be taken are flat field images. These images are needed because not every pixel is equally sensitive to the light shining on them due to the mass production of pixel elements. Another reason why flat fields are necessary is due to dust specks on the CCD faceplate and filters. The dust causes every image to have dark “doughnuts” on them. The doughnut shape of the dust specks occur due to the fact that they are not in focus. IRAF averages the output of the pixels to create a master flat frame. However, since light reaches the chip the observer produces flat-fields for every color of the planned observation. These master flats are then divided into the difference between the object and the bias frame so that the equation to reduce an image is:

$$\text{Reduced Image} = [\text{Object} - \text{Bias} - (\text{dark-bias})] / \text{Flat} \quad 1$$

the dividing is done to make the background of the reduced image as uniform as possible. There are two ways of taking a flat field image. The first involves a large, flat screen that is illuminated. The idea here is that the screen will provide a uniform intensity for all the pixels to determine which pixels are more sensitive in each filter. The biggest problem is actually trying to provide uniform illumination on the screen. However, the



advantage here is that it can be performed at any time during the observation run, multiple times if need be. The other way of getting flat-frames is to point the telescope toward the twilight sky and take the flats-fields that way. The idea here is to use the small field of view for most CCD cameras to create an image of the sky that is nearly uniform in intensity. The main disadvantage of this method is that more care must be taken due to the small window of opportunity that is allowed before it gets too dark and stars begin to populate the field. Thus, if this window is missed, the observer must wait till morning twilight before getting another chance for flats.

## **Photometry**

After the reduction of the object frames the next step would be to extract the useful data from the images. CCD Photometry is essentially taking the number of counts received on the CCD chip and converting it to an instrumental magnitude. The equation that will be used to do this is:

$$v = -2.5 \text{Log}(N_c) \quad \mathbf{2}$$

where  $N_c$  is the number of counts detected per unit time and  $v$  is the measured instrumental magnitude. Before that can be done there is one more correction that has to be made. Even though most of the counts from a star originate from the light hitting the CCD chip there is still a little bit of extra

light that arises from the sky background. What is done in photometry is to draw a circle around the star, an annulus for the sky sample, then take the measurements. The number of counts per unit time inside the circle represents the star plus the sky while the annulus provides an average sky count. This average is then subtracted from the star + sky count to get the number of counts from the star. After measuring  $N_c$ , Equation 2 is used to calculate the instrumental magnitude for the star.

## **Differential Photometry**

Differential photometry is a technique in which the amount of light from the variable is subtracted by the light from a nearby comparison star. This type of work it is useful for a couple of different reasons. The first being that the sky need not be completely clear and stable in order to get useful data. Any changes that occur in sky conditions will affect all stars in the field of view so long as the field of view is small and exposure times are long. This is particularly useful in places that often experience poor sky conditions. The other advantage is that differential photometry is more precise by picking up small variations that the variable star might undergo during an observation. For further redundancy, a check star is usually observed in the star field. The role of the check star is to make sure that the

comparison star is not itself a variable star simply by taking the light from the comparison star and subtracting the light from the check star.

## **Extinction**

If the goal is to convert the magnitudes to a standard system of magnitudes, then the observer must make still more corrections to the data. One correction arises because Earth has an atmosphere. As light passes through Earth's atmosphere the light is scattered and absorbed. It is the very reason why the sky is blue overhead and gradually becomes a whitish color as one looks closer to the horizon during the day. The extinction is also a property of the sky conditions such as the humidity and the amount of air between the observer and the object. This means extinction changes from night to night as well as throughout the night as the star moves across the sky. Contrast this with the bias, flat, and dark frames that are inherent in the CCD camera being used and are more or less be constant. The basic equation for determining the extinction is given by:

$$m_{\lambda_0} = m_{\lambda} - (k'_{\lambda} + k''_{\lambda} c)X \quad \mathbf{3}$$

where  $m_{\lambda}$  is the magnitude that would be measured if above Earth's atmosphere,  $k'$  is the principal extinction coefficient,  $k''$  is the second order extinction coefficient,  $c$  is a measured color index and  $X$  is the air mass. Air

mass is simply the mass of air that lies between the observer and the star and so long as the star is somewhat high in the sky the air mass is approximated to be:

$$X = \text{Sec}(Z) \quad 4$$

where  $Z$  is the angle between the zenith and a line that extends from the observer to the star.

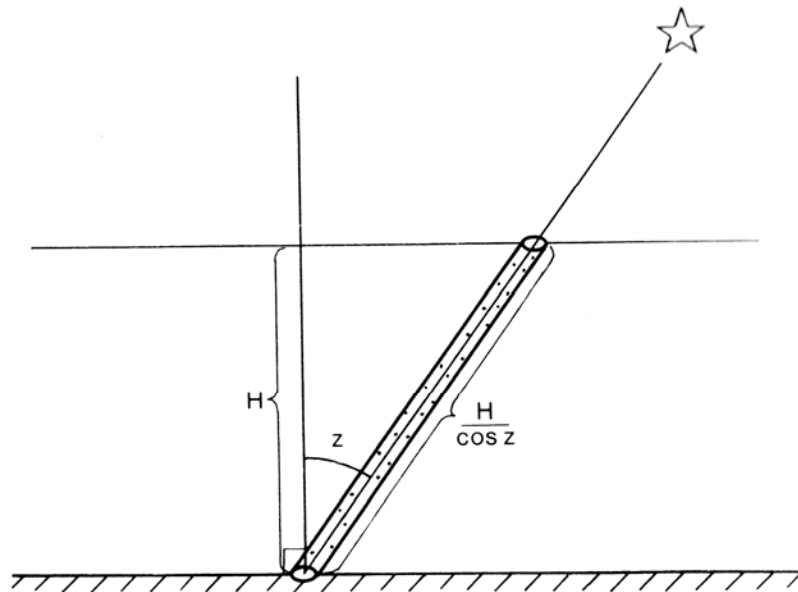


Figure 9: Diagram of how air mass is calculated. This approximation works for  $Z = \pm 60$  degrees [Karttunen et al. 2000]

Usually  $k''$  is a very small value and can be neglected, so setting  $k''$  to zero and solving Equation 3 for  $m_\lambda$  produces:

$$m_\lambda = k'_\lambda X + m_{\lambda 0} \quad 5$$

Equation 5 is the equation for a straight line. In order to find the extinction coefficient simply graph the instrumental magnitude (which has now been measured) vs. the air mass (which is recorded as the data are taken). The slope of the line that best fits the data will be the extinction

coefficient. The point where the line intercepts the y-axis will be the magnitude of the star if there was no atmosphere, which would be an air mass of zero.

The best stars to use in determining the extinction coefficient are bright stars that are already in the field of interest. The reasoning behind this is that the distance between the star used to determine the coefficient and the star of scientific interest is very small, usually on the order of arcseconds. Since this distance is small it can be assumed that the extinction correction will be the same for both stars. The extinction coefficient is of course wavelength dependant and explains why we have different colors of sky at different parts of the day, and therefore must be computed for each filter that is being used.

## **Transformation Coefficient**

If two astronomers, studying the same star but using different equipment setups, compare their instrumental magnitudes they would find their numbers could vary drastically. This is due to different equipment and how they are calibrated. In order for astronomers to compare their data they must be transformed to a standard magnitude system. The magnitude system

used in this work is the Bessel BVRI system. The transformation for the visual filter is given by:

$$V = v_0 + \varepsilon(B - V) + \zeta_v \quad \mathbf{6}$$

where  $V$  is the standardized magnitude,  $v_0$  is the instrumental magnitude. The two other terms in the equation,  $\varepsilon$  and  $\zeta$  are the transformation coefficient and zero point respectfully. Both of these terms have to be determined. We start by rearranging the Equation 6 as follows:

$$V - v_0 = \varepsilon(B - V) + \zeta_v \quad \mathbf{7}$$

once again this resembles the equation of a straight line where the slope of the line is the transformation coefficient and the y-axis intercept is the zero point. The problem here is that we know neither  $V$  nor  $B - V$ . It is this point that standard stars are used. Standard stars are useful because their standardized magnitudes and colors are already known. Their values are listed in tables and are referred to during this process. Since their values are known, the unknown values in Equation 6 can be found by plotting  $V - v_0$  vs.  $B - V$  for several standard stars or clusters of stars that have a wide variety of values.  $V$  and  $B - V$  are the values associated with the standard stars, which are referenced, and  $v_0$  is already known from the photometry of the standard stars via direct observation of the equipment used to study the objects of study. These data points are plotted and a best-fit line is computed where the

slope becomes the transformation coefficient and the zero point corresponds to the y-axis intercept.

Knowing all the values for Equation 6 one can then transform the instrumental magnitudes into standard magnitudes for the visible filter. The other filters in the BVRI system are treated in the same fashion and the equations are similar and can be used just as easily.

## **Blackbody Fitting**

A blackbody is a theoretical object that absorbs all light that is incident upon it while reflecting no light in return. The light that is re-emitted from this object is dependent on the temperature such that higher temperature objects will be bluer in color and vice versa. The obvious benefit to this is that blackbody fitting can be used to determine the temperature of an object. For this research the temperature of the disk can be examined to see how, and if, it changes throughout the observing session. How the disk changes during an outburst is inferred from the data. The starting point will be with the relation:

$$\frac{F_{(\lambda)Obs}^L}{F_{(\lambda)Obs}^E} = \frac{F_{(\lambda)Calc}^L}{F_{(\lambda)Calc}^E} \quad \mathbf{8}$$

where L and E denote later and earlier times respectively and Obs and Calc are observed and calculated fluxes at any time. We may assume that all the light that is observed as coming from the disk. The justification for this is the fact that the disk is much brighter than the secondary. And although the white dwarf is hotter than the disk, its small size would not contribute much to the overall light output. The right side of Equation 8 can be rewritten as the following:

$$\frac{F_{(\lambda)Calc}^L}{F_{(\lambda)Calc}^E} = \frac{A^L I_{\lambda}(T_{eff}^L) D_L^2}{A^E I_{\lambda}(T_{eff}^E) D_E^2} \quad \mathbf{9}$$

with A being surface area of the object, i.e. the disk, I is the intensity as a function of the effective temperature and wavelength, and D being the distance to the object. It is a reasonable assumption that the distance will be a constant during the observations so they will cancel out in the ratio giving the following:

$$\frac{F_{(\lambda)Obs}^L}{F_{(\lambda)Obs}^E} = \frac{A^L I_{\lambda}(T_{eff}^L)}{A^E I_{\lambda}(T_{eff}^E)} \quad \mathbf{10}$$

Therefore, if one knows the ratios of the observed fluxes and the intensities, then the behavior of the surface areas can be determined. Using the above equation we work on the left side of the equation, as it is easier. Because flux and magnitude are related the flux ratio easily becomes:



$$\frac{F_{(\lambda)Obs}^L}{F_{(\lambda)Obs}^E} = 10^{-0.4(V_0 - V_t)} \quad \mathbf{11}$$

The naught denotes an earlier time and t as a later time. The earlier time will be the beginning of the night and will be the basis of comparison as the area changes throughout the outburst. However, temperature is still unknown at this point. This can be determined by using the right hand side of Equation 10. For the intensity we use the Plank Blackbody equation which is given as:

$$I_{\lambda}(T_{eff}) = \frac{8\pi hc}{\lambda^5} \left[ \frac{1}{e^{\frac{hc}{\lambda kT}} - 1} \right] \quad \mathbf{12}$$

Using Equation 12 for two different colors, visual and red for example, and canceling constants one obtains the following relationship:

$$\frac{I_v(T_{eff})}{I_R(T_{eff})} = \left( \frac{\lambda_v}{\lambda_R} \right)^5 \left[ \frac{e^{\frac{hc}{\lambda_R kT}} - 1}{e^{\frac{hc}{\lambda_v kT}} - 1} \right] \quad \mathbf{13}$$

This equation would be rather cumbersome to solve for T, but it's possible to determine T numerically. It is possible because we know the wavelengths of the observations, and when a ratio is taken we know the left side of the flux ratio will become  $10^{[-0.4(V - q_v - R + q_r)]}$  with  $q_v$  and  $q_r$  being a pre-selected flux of a star with zero magnitude. This yields the equation:

$$10^{-0.4(V - q_v - R + q_r)} = \left( \frac{\lambda_R}{\lambda_v} \right)^5 \left[ \frac{e^{\frac{hc}{\lambda_v kT}} - 1}{e^{\frac{hc}{\lambda_R kT}} - 1} \right] \quad \mathbf{14}$$

The only unknown in Equation 14 is the temperature. Therefore in order to find temperature, reasonable values for T are plugged in until the right side equals the left side.

With the temperature known at a particular time, the intensity ratio from Equation 10 can be determined for a single wavelength using Planck's equation above. Finally, the area ratio in Equation 10 is solved to determine if there was any change to the disk area during the outburst.

# Results

## CN Orionis

CN Orionis (CN Ori) is a Z Cam type cataclysmic variable star in the constellation of Orion. During quiescence it has a visual magnitude of 16.2, which can brighten to a visual magnitude of 11 during an outburst [CGCVS]. The system experiences an outburst, on average, every 18 days. CN Ori has an orbital period of about 0.16 days and exhibits a sinusoidal light curve, which suggests an eclipse during the orbit [Mumford 1967].

A comprehensive and ambitious study conducted by Schoembs in 1981 attempted to create a continuous light curve of CN Ori by utilizing three telescopes to keep track of the star as it progressed through its outburst cycle. According to the paper, bad weather prevented two of the telescopes from taking part in the study. The result is an impressive, yet still incomplete, 15-day light curve of the system from outburst, through quiescence, and back into outburst. Schoembs shows that no matter where in the cycle CN Ori happens to be it shows periodic light variation [Schoembs

1982]. The study however, was only done in visible whereas this study is in four colors and uses far less data.

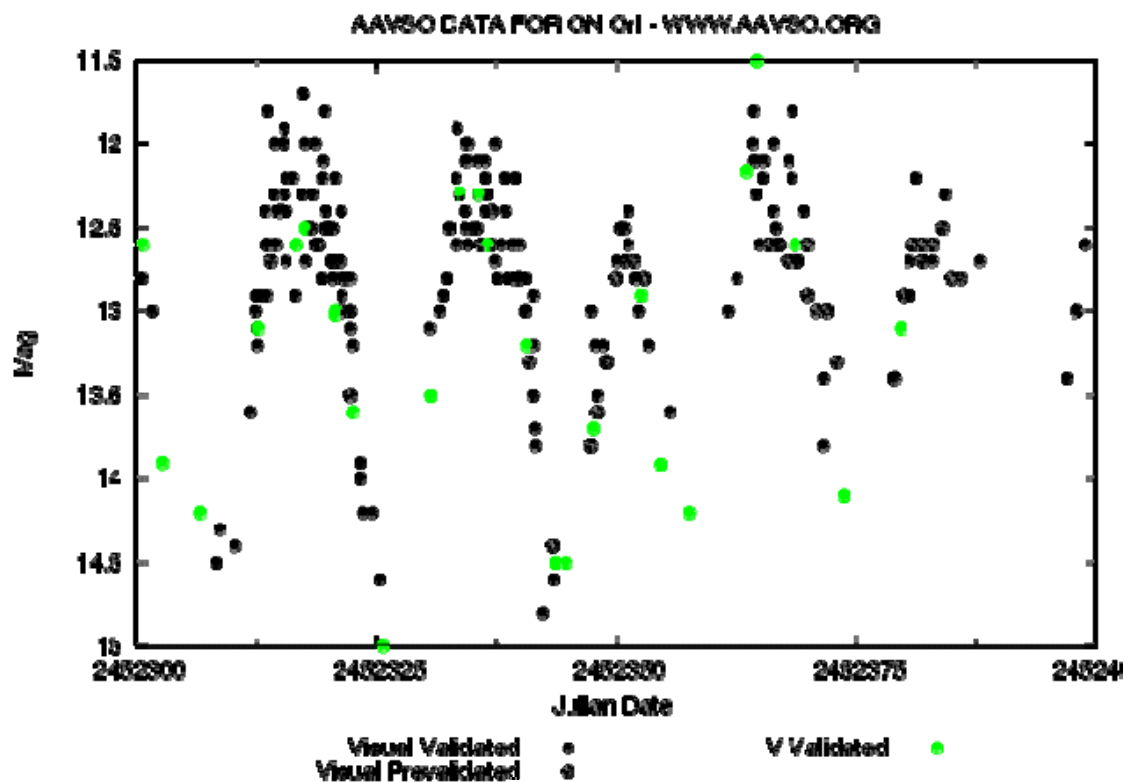


Figure 10: One hundred day light curve of CN Ori

## Observations

Observations of CN Ori were taken in February of 2002 at the National Undergraduate Research Observatory (NURO) near Flagstaff, AZ. The telescope has a 31-inch, F15.7 Cassegrain. It had a 512x512 pixel, nitrogen cooled Photometrics Star1 CCD camera in the BVRI color bands.

Standard stars were used to calibrate and standardize the observations of the variable and the two comparison stars. IRAF was used to reduce the data and third party software was used to perform the photometry.

## **Differential Photometry**

Figures 11 through 14 show the plots of differential magnitude vs. time from observations made on February 6<sup>th</sup>. The most obvious feature common among the graphs is their sinusoidal shape, which arises from the motion of the two stars around one another where one wavelength on the graph would equal the orbital period of the system. It appears that the system completed one period during the night, roughly 0.163 days. However the maximums are not equal, being about 0.1 magnitude different. This shows that CN Orionis was brightening during the time of data collection. The 0.163-day period corresponds to the orbital period of the system. [Schoembs 1982] In order to determine if CN Orionis was experiencing a superoutburst one would need at least several orbital periods. The data that has been gathered appears to be insufficient to make that judgment in this study.

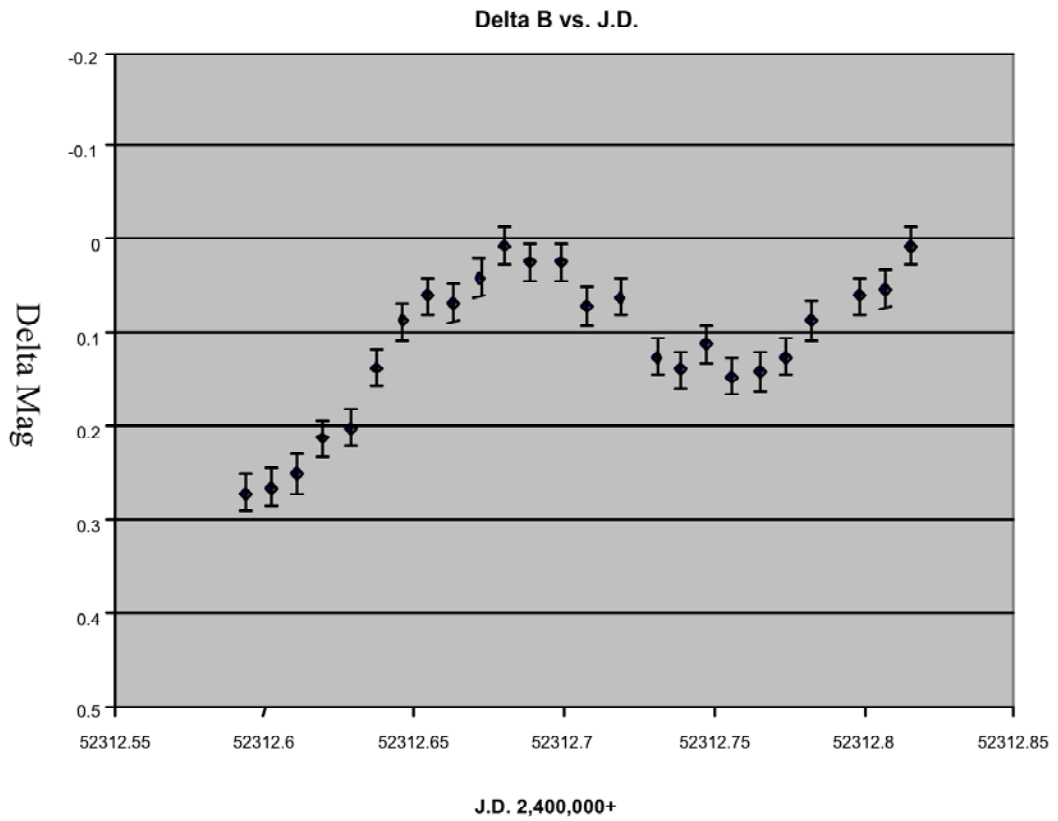


*Figure 11: Difference of variable and comp star for blue filter vs. time*

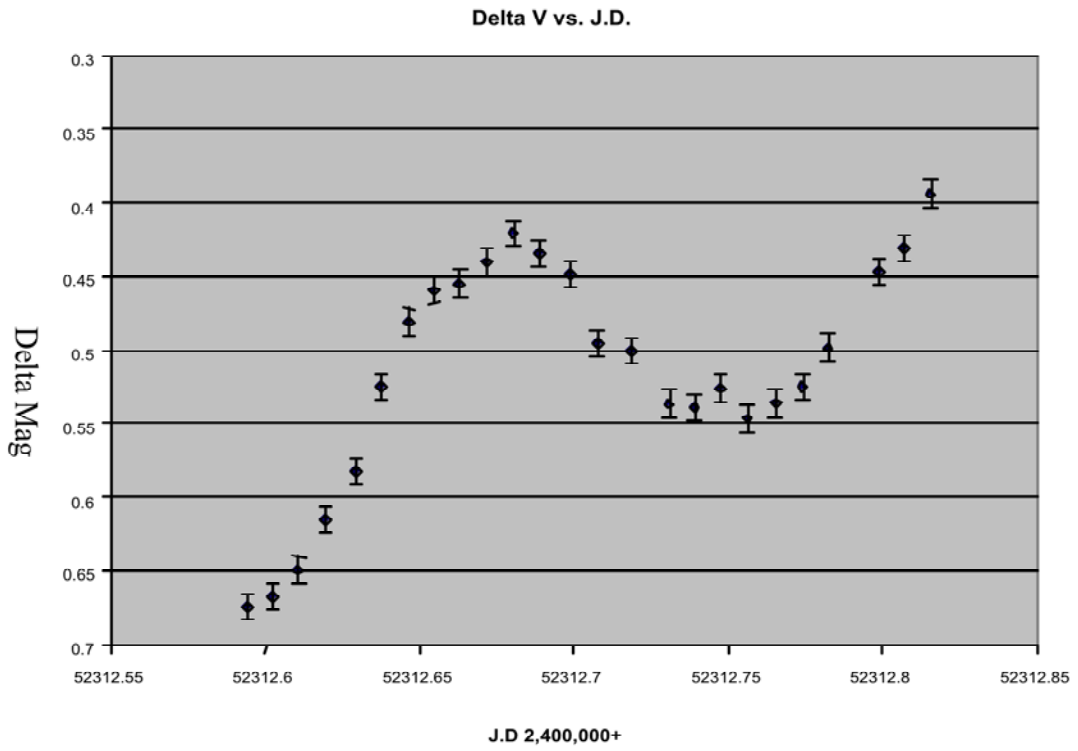
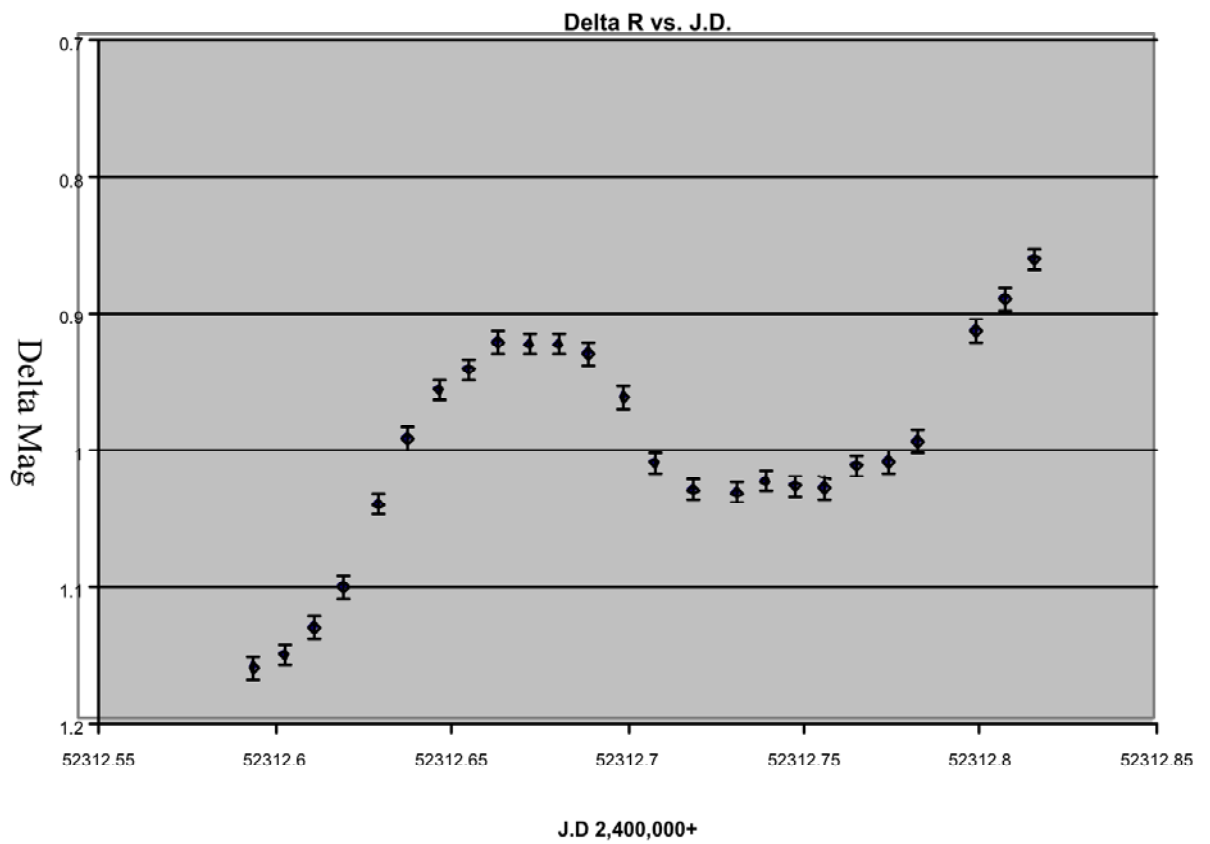
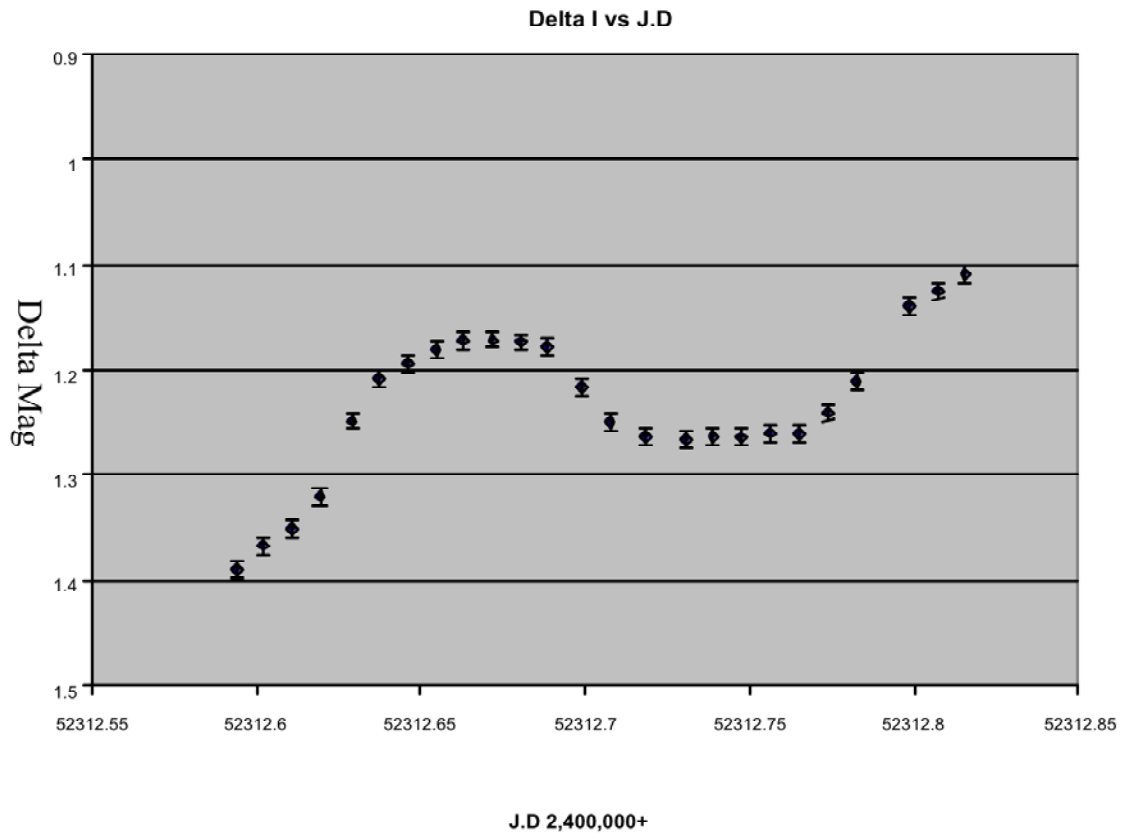


Figure 12: Delta V vs. JD







*Figure 14: Delta I vs. JD*

As the graphs show there is a sinusoidal feature through the night that is in agreement with Schoembs (1982). An interesting feature that is found is a plateau that occurs at the local minimum later in the observations. It is obvious in the R and I and possibly in the B and V observations. The nature of the plateau is unknown. An explanation might be related to the geometry of the system while in outburst or some mechanism in the disk that prevents any significant light changes from occurring at this time.

## Temperature

From the analysis of the blackbody temperatures discussed in the chapter on blackbody fitting, we can see how the temperature of the system evolves over time. From this it can be determined if a change in temperature throughout the night resulted in the increase of brightness. To determine the temperature a program written by Dr. Kaitchuck of Ball State University using the STEPIT subroutine out of Indiana University was used [Chandler 1969]. This program used three color indices (B-V, V-R, and R-I) and performs a least squares solution for a blackbody. A blackbody solution can be assumed because the disk is optically thick and approximates a blackbody.

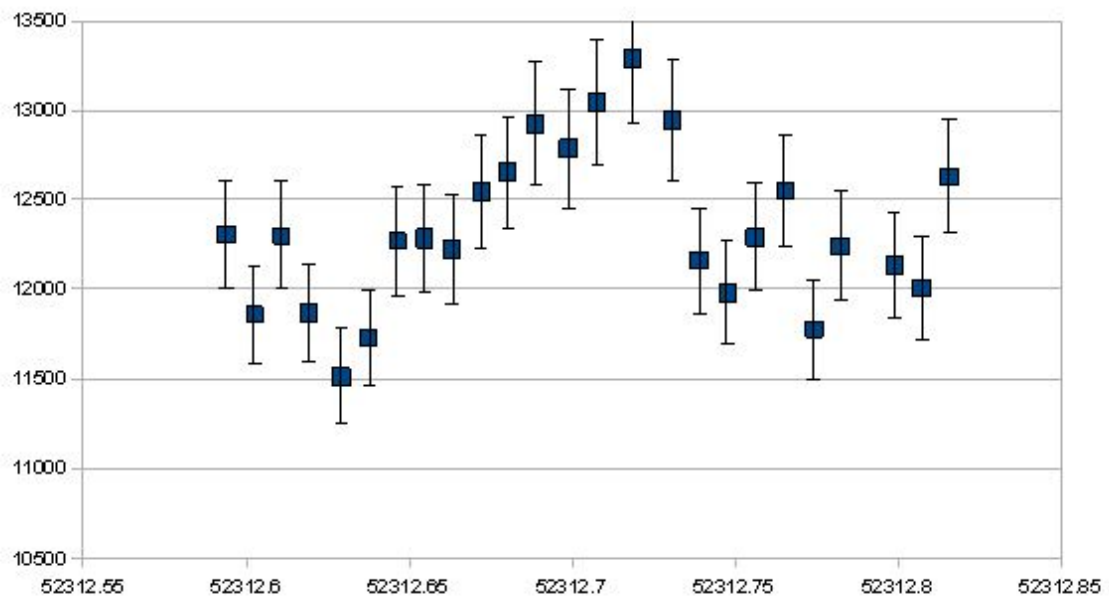


Figure 15: Temperature vs. Time

Figure 15 shows that the temperature, measured in Kelvin, has a crude sinusoidal pattern that occurs throughout the night. The graph also indicates that the change in temperature is about 1000 K before returning to about 12000 K by the end of the observations. If compared with Figures 11-14, the highest temperature corresponds to the start of a local minimum. This feature may be explained by secondary irradiation. The side of the secondary closest to the observer is a little hotter, and thus more luminous, due to the radiation of the primary passing in front of it. Alternatively, the hot spot of the disk could explain the graph as well. The hottest part of the graph relates to when the hot spot, the point on the disk where the stream of material from the secondary enters the disk, is at the highest visibility. Therefore, there would be more light and higher temperatures observed.

## **Area Ratio**

Figure 16 shows the area ratio for the night of February 6<sup>th</sup>. As discussed earlier the area ratio compares the ratios of later and earlier times, therefore the first data point will always be 1. Any area ratio that is greater than one means that the disk has grown, conversely a number less than one means the disk has shrunk over time.

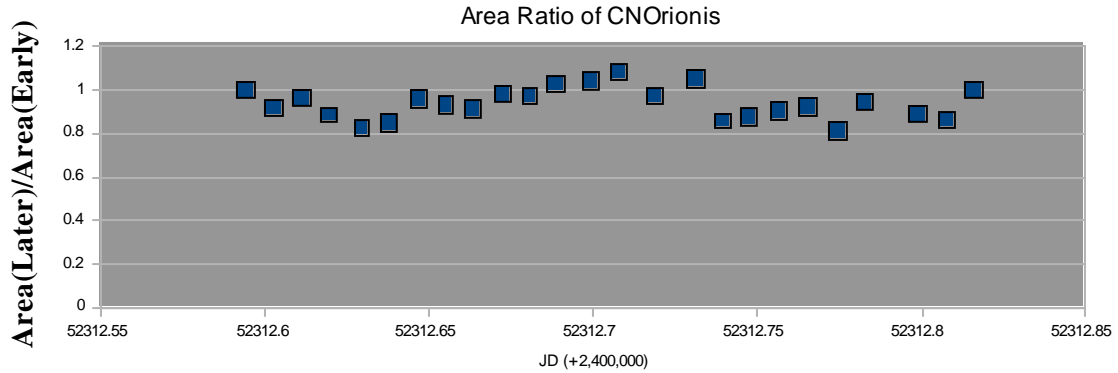


Figure 16: Disk area ratio for the night of February 6<sup>th</sup>. Error bars are comparable to the size of the data points.

Figure 16 suggests that that area of the disk changed significantly throughout the observation period. This implies that the change of the area, along with the temperature did contribute to the light variation found within the system. The graph also shows a sinusoidal pattern of the area. Figure 16 shows that the change in the area was rather significant, dropping 0.2 or about 20 percent at the beginning of the observations. The instability model does not suggest that the disk should be oscillating in size. That is the wavelength of the graph is similar to that of the orbital period of the system, it could be something related to that, or possibly an inclination of the disk and we are seeing more and less of the disk throughout the orbit.

## Conclusions

What can be said of CN Ori is that it was undergoing an outburst on the night of observation. This is shown as the upward trend in the differential photometry graphs (Figures 11-14). Figures 11-14 also confirm earlier work about CN Ori's light variability. Figure 10 would indicate that the outburst was normal and not a superoutburst. This should be treated with some caution as the orbital period of the system is about four hours long, a change of a few percent equates to less than 10 minutes. Therefore, no real conclusive evidence can be stated for certain concerning a superoutburst.

The temperature of the disk during the outburst shows a variation with time and is a contributing factor for the increase in CN Ori's light variability. The two possible explanations for the temperatures change, being the hotspot or secondary irradiation, are inconclusive due to a lack of orbital phase data.

The area graph suggests that the area of the disk did change in size overall during the outburst. The sinusoidal pattern that is seen leads us to a change in the projected area of the disk and thus would be a cause for the light variability along with temperature changes. Comparing the temperature and the area ratio graph does appear to give some correlation. However,

nothing conclusive can be reached due to the scatter of the data. The measurement of the disk's temperature changing through the night is also a first for the system.

Further study of CN Ori would include performing the same observation run that was conducted by Schoembs. The difference would be using standardized photometric observations. This would yield a more general idea on the behavior of CN Ori during all stages of its outburst cycle.

## Bibliography

- [Barreral and Vogt 1989] H. Barreral and N. Vogt, *Astronomy and Astrophysics*, **220**, 99 (1989)
- [Bessell 1990] M.S. Bessell, *Astronomical Society of the Pacific*, **102**, 1181
- [Cannizzo and Kaitchuck 1992] John K. Cannizzo and Ronald H. Kaitchuck, *Accretion Disks in Interacting Binary Stars*, *Scientific America*, January 1992 92-99
- [CGCVS] Combined General Catalogue of Variable Stars  
<http://www.sai.msu.su/groups/cluster/gcvs/gcvs/>
- [Chandler 1969] Chandler, J. P. *Behavioral Science*, **14**, 81-82
- [Cornell 2009]  
[http://www.astro.cornell.edu/academics/courses/astro201/roche\\_lobe.htm](http://www.astro.cornell.edu/academics/courses/astro201/roche_lobe.htm)
- [Hellier 2001] Coel Hellier, *Cataclysmic Variable Stars: How and why they Vary* (Praxis Publishing Ltd. 2001)
- [Henden and Kaitchuck 1982] Arne A. Henden and Ronald H. Kaitchuck, *Astronomical Photometry* (Van Nostrand Reinhold Company 1982)
- [Howell 2000] Steve B. Howell, *Handbook of CCD Astronomy* (Cambridge University Press 2000)
- [Karttunen et al. 2000] Hannu Karttunen, Pekka Kröger, Heikki Oja, Markku Poutanen, Karl Johan Donner, *Fundamental Astronomy 3<sup>rd</sup> edition* (Karttunen 2000)
- [Lipkin et al. 2001] Y. Lipkin, E.M. Leibowitz, A. Retter, O. Shemmer, *Monthly Notices of the Royal Astronomical Society*, **328**, 1169 (2001)
- [Mineshige 1983] S. Mineshige, Y Osaki, *Astronomical Society of Japan*, **35**, 377 (1983)

[Mumford 1967] G. Mumford *Publications of the Astronomical Society of the Pacific*, **79**, 283

[Osaki 2004] Y. Osaki and F. Meyer, *Astronomy and Astrophysics*, **401**, 325 (2004)

[Ritter 1997] H. Ritter and U. Kolb, *Astronomy and Astrophysics Supplemental Series*, **129**, 83 (1997)

[Schoembs 1982] R. Schoembs, *Astronomy and Astrophysics*, **115**, 190 (1982)

[Smak 1984] J. Smak, *Astronomical Society of the Pacific*, **96**, 5

[Smak 2004] J. Smak, *Acta Astronomica*, **54**, 181 (2004)

[Smak 2009] J. Smak, *Acta Astronomica*, **59**, 1 (2009)

[Warner 2003] Brian Warner, *Cataclysmic Variable Stars* (Cambridge University Press 2003)

[Zeilik and Gregory 1998] Michael Zeilik and Stephen A. Gregory, *Introductory Astronomy and Astrophysics 4<sup>th</sup> Edition* (Saunders College Publishing 1998)